Optical potential approach to K^+d scattering at low energies

Takashi Takaki*

Department of Economics, Management and Information Science, Onomichi University, Hisayamada 1600, 722-0021 Onomichi, Japan

(Received 16 December 2009; published 14 May 2010)

I study K^+d scattering at low energies using optical potential. My optical potential consists of the first- and second-order terms. The total, integrated elastic, and elastic differential cross sections at incident kaon momenta below 800 MeV/c are calculated using my optical potential. I found that my results are consistent with the Faddeev calculation as well as the data and especially that the second-order optical potential is essential for reproducing them at low energies. I also discuss the multiple scattering effects in this process.

DOI: 10.1103/PhysRevC.81.055204 PACS number(s): 25.80.Nv, 13.75.Jz, 14.40.Df, 24.10.−i

I. INTRODUCTION

One of the important purposes for studying K^+d scattering is to understand the K^+N interaction because the isospin zero-K^+N amplitude or K^+-neutron amplitude can be obtained only through K^+d scattering. Recently, some experimental studies [1,2] have suggested that the pentaquark resonance $\Theta(1540)$ with a narrow width might be excited in this isospin channel, although its existence has not been confirmed yet. Because the K^+ meson is built from a $u\bar{s}$ quark state, it cannot form the conventional three-quark resonance with a nucleon. So the pentaquark resonance must have an exotic structure such as a $uudd\bar{s}$ quark state, and the coupling with the K^+N system is expected to be weak. In fact, the width of the $\Theta(1540)$ has been found to be less than 1 MeV [3–5] through the analysis of the K^+d reaction. Therefore, the K^+N system is a weaker interacting system than other meson-nucleon systems such as $\pi^\pm N$ and K^-N, which have the strong couplings with resonant particles. K^+d scattering at low energies is much simpler than $\pi^\pm d$ and K^-d scatterings because the pion absorption in $\pi^\pm d$ scattering and the conversion to $\pi N\Lambda$ and $\pi N\Sigma$ in K^-d scattering occur even at the threshold. At incident kaon momenta below 600 MeV/c, where the pion production does not occur, the K^+d system has only three reactions: the elastic scattering $K^+d \to K^+d$, the breakup reaction $K^+d \to K^+pn$, and the charge exchange reaction $K^+d \to K^0pp$. Thus, the analysis of the K^+d scattering at low energies is suited to examining rigorously the validity of various theoretical models [5–9]. One of them is the three-body calculation using the Faddeev method [8,9], where the multiple scattering effects have been estimated accurately.

Because of the weak K^+N interaction, the single scattering impulse approximation, where one nucleon in the deuteron is regarded as a spectator, is able to describe successfully the total cross sections at incident momenta ($P_{\rm lab}$) above ∼500 MeV/c [6,8]. Furthermore, the elastic differential cross sections at the low-momentum transfer can be explained even at lower energies. However, the single scattering impulse approximation explicitly violates the unitarity at incident momenta below ∼200 MeV/c; that is, the integrated elastic cross section is larger than the total cross section that is obtained via the optical theorem [8] and fails to describe the suppression of the breakup differential cross section at the forward kaon scattering angles [9]. This means that additional mechanisms are needed to remedy such situations.

It was pointed out in Ref. [4] that the effect of the kaon rescattering can resolve the discrepancy owing to the violation of the unitarity. Actually, its effect increases the total cross section significantly at incident momenta below ∼400 MeV/c. In this calculation, however, the static nucleon approximation was used. The large mass of the kaon suggests that the nucleon recoil effect is important. So the nonstatic treatment may be necessary to get a reliable result. Then it was found [9] that the discrepancy about the breakup differential cross section can be resolved by the nucleon-nucleon (NN) interaction effect and specifically the suppression is attributable to the orthogonality between the NN final-state continuum wave function and the deuteron wave function. A recent article [7] has shown that the NN final-state interaction (FSI) plays an essential role in the reduction of the integrated breakup cross sections and decreases the total cross sections largely in the momentum range from 50 to 800 MeV/c. As a result, their calculations with FSI on the total cross sections are consistent with the data. However, their results are in conflict with those of other works [6,8], which show that the total cross sections above ∼500 MeV/c can be reproduced with the single scattering impulse approximation as already mentioned. These facts indicate that the effects of both kaon rescattering and NN interaction should be included in a theory and also that a more careful treatment is necessary to describe the K^+d scattering consistently at low energies.

In this article I investigate the K^+d scattering using the optical potential defined in the multiple scattering theory of Watson [10]. My optical potential consists of the first-order and second-order terms. The second-order optical potential is constructed to include multiple scattering corrections such as the kaon rescattering, the Pauli correction and the NN interaction. One of the features of this approach is that it does not violate the unitarity. Furthermore, because this formulation has a simple structure, the calculation is more easily performed than the Faddeev calculation. I examine how my optical potential works for the K^+d scattering and demonstrate the importance of the multiple scattering effects. To do so, I calculate the energy dependence of the total cross sections, integrated reaction cross sections, and elastic cross

*takaki@onomichi-u.ac.jp

sections and then compare my calculations with the data. I show that my approach predicts the data as well as the Faddeev method and especially that the second-order optical potential is needed to describe both the data and the Faddeev calculation at low energies. Indeed, the cross section calculated with only the first-order optical potential is not consistent with the Faddeev calculation at low energies despite the weak K^+N interaction. The present work is the first application of the optical potential including the second-order term to the K^+d scattering. The optical potential up to second order is also obtained from the Kerman-McManus-Thaler (KMT) [11] theory. I will discuss the relation between my approach and the KMT one. In the analysis of the meson-nucleus scattering, the first-order optical potential has been usually used. The results of this work could provide useful information about the role of the second-order optical potential in the K^+-nucleus scattering.

The article is organized as follows: I present my formalism in Sec. II. In Sec. III I show my calculations for the total, elastic, and inelastic cross sections and compare them with the data and the Faddeev calculation. In Sec. IV I summarize my work.

II. FORMALISM

A. Outline of the optical potential approach

To calculate the cross sections of the K^+d scattering, I use the optical potential derived from the multiple scattering theory. There are two formulations for the multiple scattering theory, that is, the Watson [10] and the KMT [11] theories. Although they have different forms, they are identical in content. In this work, I employ the Watson theory because the physical interpretation of the optical potential is clear. My optical potential will be constructed to incorporate the multiple scattering corrections such as the rescattering, the Pauli effect, and the NN interaction. To do so, the second-order optical potential is considered in addition to the usual first-order optical potential. I start by briefly reviewing the Watson formulation.

For the scattering of a positive kaon from A identical nucleons, the transition amplitude T is a solution of the Lippmann-Schwinger equation,

$$T = \sum_{i=1}^{A} v_i + \sum_{i=1}^{A} v_i \frac{\mathcal{A}}{e} T, \tag{1}$$

where

$$e = E - K_0 - H_A + i\epsilon. \tag{2}$$

Here E is the total energy, K_0 is the kaon kinetic energy, and H_A is the Hamiltonian of the target nucleus. The two-body potential v_i describes the interaction between the kaon and ith nucleon. $\mathcal{A}$ is a projection operator onto the antisymmetric subspace of the Hilbert space. As far as one works in the antisymmetric subspace, the operator $\mathcal{A}$ is not necessary in Eq. (1) because T and $\sum_{i=1}^{A} v_i$ are symmetric operators. For later convenience, however, it is inserted explicitly in Eq. (1).

Now I introduce a projection operator P, which projects onto the nuclear ground state, and Q is defined by

$$Q = \mathcal{A} - P. \tag{3}$$

Using these operators, Eq. (1) is rewritten in terms of the optical potential U as

$$T = U + U \frac{P}{e} T, \tag{4}$$

where U is given by

$$U = \sum_{i=1}^{A} U_i, \tag{5}$$

with

$$U_i = \widehat{t}_i + \widehat{t}_i \frac{Q}{e} \sum_{j \neq i} U_j. \tag{6}$$

The kaon-nucleon T matrix $\widehat{t}_i$ in Eq. (6) is defined by

$$\widehat{t}_i = v_i + v_i \frac{Q}{e} \widehat{t}_i. \tag{7}$$

To evaluate the optical potential U, I define another kaon-nucleon T matrix t_i such that

$$t_i = v_i + v_i \frac{1}{e} t_i, \tag{8}$$

where the kaon propagates in the space of both antisymmetric and non-antisymmetric states of the nucleus. The relation between many-body operators $\widehat{t}_i$ and t_i is

$$\widehat{t}_i = t_i - t_i \frac{1 - \mathcal{A} + P}{e} \widehat{t}_i. \tag{9}$$

Here the operator $1 - \mathcal{A}$ projects onto the Pauli-violating states. The second term of Eq. (9) appears to remove the contribution of the transition to the Pauli-violating states and the ground state from t_i. If the term proportional to P is neglected, the coherent rescattering is overcounted in the calculation of Eq. (4).

Before constructing my model, let us discuss the relation between the Watson and KMT formulations. In the KMT theory (see the Appendix), the following many-body operator τ_i is used to define the optical potential,

$$\tau_i = t_i - t_i \frac{1 - \mathcal{A}}{e} \tau_i, \tag{10}$$

where the projection operator P does not appear because the coherent rescattering is counted in a different way. The relation between the operators $\widehat{t}_i$ and τ_i is given by

$$\widehat{t}_i = \tau_i - \tau_i \frac{P}{e} \widehat{t}_i. \tag{11}$$

The first-order optical potentials are given by $\sum_{i=1}^{A} \widehat{t}_i$ for the Watson approach and $\frac{A-1}{A} \sum_{i=1}^{A} \tau_i$ for the KMT approach, respectively. Within this first-order expansion, the two approaches give identical transition amplitude, as pointed out in Ref. [12]. Even if further approximations are assumed, this is still correct as far as the relation (11) holds. In the actual calculations, however, one usually uses the impulse approximation where $\widehat{t}_i$ and τ_i are replaced by the free

two-body T matrix $t_i^{\rm free}$. In this case, the relation (11) does not hold and therefore the two approaches give different transition amplitudes. In fact, it has been shown in the studies [13,14] of the pion-deuteron scattering that the KMT first-order optical potential is superior to the Watson one. So it is necessary to go beyond the first-order optical potential in the impulse approximation and take into account the second term of Eq. (9) to get the reliable results within the Watson formulation. There are several models taking account of this term. In the delta-hole model [15], the second term of Eq. (9) is incorporated by adding a Fock term to the delta-hole propagator. In the model of Ref. [12], the channel-coupled equations are derived from Eq. (9) and are solved to get the first-order optical potential. In this work, I expand the T matrix $\widehat{t_i}$ of Eq. (9) in terms of t_i and consider it to second order.

Now I construct the optical potential which will be used in my calculations. By substituting Eq. (9) into Eq. (6), the optical potential U can be given in terms of t_i by

$$U = \sum_i t_i - \sum_i t_i \frac{1-\mathcal{A}+P}{e} t_i + \sum_{i\neq j} t_i \frac{Q}{e} t_j + \cdots \tag{12}$$

$$= \sum_i t_i + \sum_{i\neq j} t_i \frac{1}{e} t_j - \sum_{i,j} t_i \frac{P}{e} t_j - \sum_{i,j} t_i \frac{1-\mathcal{A}}{e} t_j + \cdots, \tag{13}$$

which is explicitly written up to second order in t_i. Note that the fourth term of Eq. (13), describing the transition to the Pauli-violating states, are omitted hereafter because the matrix element of this term between the nuclear antisymmetric ground state vanishes.

I now consider the deuteron as the target nucleus and introduce additional approximations to derive the optical potential in my approach. In the impulse approximation, t_i $(i = 1, 2)$ is replaced with the free two-body T matrix $t_i^{\rm free}$ defined by

$$t_i^{\rm free} = v_i + v_i \frac{1}{e_0} t_i^{\rm free}, \tag{14}$$

with

$$e_0 = E - K_0 - K_1 - K_2 + i\epsilon, \tag{15}$$

where K_i $(i = 1, 2)$ is the kinetic energy of ith nucleon and $E - K_j$ $(j \neq i)$ is the collision energy for the kaon-ith nucleon subsystem. In my approach, the effect of the NN interaction is taken into account because it is important at low energies and, particularly, it leads to the non-negligible FSI in the breakup reaction. Because H_A in Eq. (2) is equal to $K_1 + K_2 + v_{12}$, where v_{12} is the NN interaction, the many-body Green function $1/e$ can be expressed in terms of the two-nucleon T matrix t_{NN} as

$$\frac{1}{e} = \frac{1}{e_0} + \frac{1}{e_0} t_{NN} \frac{1}{e_0}, \tag{16}$$

with

$$t_{NN} = v_{12} + v_{12} \frac{1}{e_0} t_{NN}, \tag{17}$$

where the collision energy of the two-nucleon subsystem is $E - K_0$. Thus the many-body operator t_i is expressed as

$$t_i = t_i^{\rm free} + t_i^{\rm free} \frac{1}{e_0} t_{NN} \frac{1}{e_0} t_i. \tag{18}$$

Substituting Eqs. (16) and (18) into Eq. (13) yields

$$U = U^{(1)} + U^{(2)} + \cdots, \tag{19}$$

where

$$U^{(1)} = \sum_{i=1}^{2} t_i^{\rm free}, \tag{20}$$

$$U^{(2)} = \sum_{i\neq j} t_i^{\rm free} \frac{1}{e_0} t_j^{\rm free} + \sum_{i,j} t_i^{\rm free} \left(\frac{1}{e_0} t_{NN} \frac{1}{e_0} - \frac{P}{e} \right) t_j^{\rm free}. \tag{21}$$

Here $U^{(1)}$ and $U^{(2)}$ are the first- and second-order optical potentials, respectively. The higher-order potentials are neglected in my calculation. The second-order potential consists of three terms as

$$U^{(2)} = U_d^{(2)} + U_n^{(2)} - U_c^{(2)}. \tag{22}$$

Here $U_d^{(2)}$ corresponds to the first term on the right-hand side of Eq. (21) describing the double scattering, that is, the kaon rescattering. The second term on the right-hand side of Eq. (21) is divided into two terms, that is, $U_n^{(2)}$ and $U_c^{(2)}$, which describe the effects of the NN scattering and the coherent rescattering, respectively. The quantity $U_n^{(2)} - U_c^{(2)}$ is called the modified NN scattering term in this article. The two-nucleon T matrix t_{NN} in $U_n^{(2)}$ is a function of the variable E_N, where $E_N = E - K_0 - K_{\rm c.m.}$ and $K_{\rm c.m.}$ is the kinetic energy of the center of mass of two nucleons, and has a bound state pole at $E_N = -E_B$ where E_B is the binding energy of the deuteron. Note that the propagators of $U_n^{(2)}$ and $U_c^{(2)}$ are almost identical in the vicinity of the pole at $E_N = -E_B$, that is,

$$\frac{1}{e_0} t_{NN} \frac{1}{e_0} \cong \frac{|0\rangle\langle 0|}{E_N + E_B + i\epsilon} = \frac{P}{e}, \tag{23}$$

where $|0\rangle$ is the bound-state wave function [16].

Here I consider the relation between the Watson and KMT transition amplitudes, that is, T and $T_{\rm KMT}$. Let us assume that the corresponding optical potentials are $U \cong U^{(1)} + U^{(2)}$ and $U_{\rm KMT} \cong U_{\rm KMT}^{(1)} + U_{\rm KMT}^{(2)}$ (see the Appendix), respectively. These transition amplitudes are expanded in powers of U or $U_{\rm KMT}$ as

$$T = U + U \frac{P}{e} U + \cdots, \tag{24}$$

$$T_{\rm KMT} = 2 \left(U_{\rm KMT} + U_{\rm KMT} \frac{P}{e} U_{\rm KMT} + \cdots \right). \tag{25}$$

Using the preceding equations, the amplitudes T and $T_{\rm KMT}$ can be rewritten in powers of $t_i^{\rm free}$. Then one finds the following relation:

$$T = T_{\rm KMT} + O[(t^{\rm free})^3]. \tag{26}$$

T is equal to $T_{\rm KMT}$ up to second order in $t^{\rm free}$. If the second term on the right-hand side of Eq. (26) would be small, the two approaches would give approximately the identical transition

amplitude. I have numerically checked that this is true for the K^+d scattering. Note that $T \cong T_{\rm KMT} \cong U^{(1)}$ at kaon momenta above $\sim$500 MeV/c, where the single scattering impulse approximation works well.

The purpose of this work is to evaluate the total and integrated elastic cross sections of the K^+d scattering. These are obtained by solving Eq. (4), where the optical potential U is given by Eqs. (20) and (21). The total cross section is calculated via the optical theorem as

$$\sigma_{\rm tot} = \frac{4\pi}{k} {\rm Im} f_{Kd}(\mathbf{k}, \mathbf{k}), \tag{27}$$

where the scattering amplitude f_{Kd} is given by

$$f_{Kd}(\mathbf{k}', \mathbf{k}) = -\frac{2\omega E_d}{4\pi W} \langle \mathbf{k}' d | T | \mathbf{k} d \rangle. \tag{28}$$

Here $\mathbf{k}$ ($\mathbf{k}'$) is the initial (final) kaon momentum, ω and E_d are the total energies of the kaon and the deuteron in the kaon-deuteron center of mass (c.m.) frame, and $W(=\omega + E_d)$ is the total energy of the kaon-deuteron system. The spin quantum numbers are implicitly included. The integrated elastic cross section for the unpolarized deuteron is obtained by integrating the differential cross section over the angle as

$$\sigma_{\rm el} = \int \frac{d\sigma}{d\Omega} d\Omega = \int \left(\frac{1}{3} \sum_{\rm spin} |f_{Kd}(\mathbf{k}', \mathbf{k})|^2 \right) d\Omega, \tag{29}$$

where $|f_{Kd}|^2$ is summed over the initial and final spin orientations.

B. The method of calculation

My numerical calculations will be performed in the momentum space representation. The Lippmann-Schwinger equation (4) in the kaon-deuteron center-of-mass frame is expressed as

$$\langle \mathbf{k}' d | T | \mathbf{k} d \rangle = \langle \mathbf{k}' d | U | \mathbf{k} d \rangle + \int \frac{d^3 k''}{(2\pi)^3} \langle \mathbf{k}' d | U | \mathbf{k}'' d \rangle \times G_p(W, \mathbf{k}'') \langle \mathbf{k}'' d | T | \mathbf{k} d \rangle \tag{30}$$

$$G_p(W, \mathbf{k}'') = \frac{1}{W - \omega'' - E_d(k'') + i\epsilon}. \tag{31}$$

Here the spin and isospin are omitted for simplicity. This equation is solved by decomposing into the partial waves. To calculate the optical potential $\langle \mathbf{k}' d | U | \mathbf{k} d \rangle$ given by Eqs. (20) and (21), one needs the off-shell kaon-nucleon T matrix $t^{\rm free}$ and the off-shell nucleon-nucleon T matrix t_{NN}. They are taken to be of separable form.

The kaon-nucleon T matrix in the general frame is

$$\langle \mathbf{k}' \mathbf{p}' | t^{\rm free} | \mathbf{k} \mathbf{p} \rangle = \frac{m}{\sqrt{4\omega' \omega E_{p'} E_p}} \mathcal{M}(s, \kappa', \kappa), \tag{32}$$

$$\mathcal{M}(s, \kappa', \kappa) = -\frac{4\pi\sqrt{s}}{m} f_{KN}(s, \kappa', \kappa), \tag{33}$$

where f_{KN} is the scattering amplitude consisting of the non-spin-flip and spin-flip terms, and $\mathbf{k}$, $\mathbf{k}'$, $\mathbf{p}$, and $\mathbf{p}'$ are the momenta of the initial kaon, the final kaon, the initial nucleon, and the final nucleon, respectively. Furthermore, ω, ω', E_p, and $E_{p'}$ are the energies of the initial kaon, the final kaon, the initial nucleon and the final nucleon, respectively, and m and s are the nucleon mass and the invariant mass squared of the kaon-nucleon system, respectively, and κ and κ' are the momenta of the initial and final kaons in the kaon-nucleon c.m. frame, respectively. The partial-wave amplitude $\mathcal{M}_{lj}$ is given as

$$\mathcal{M}_{lj}(s, \kappa', \kappa) = g_l(\kappa') G_{lj}(s) g_l(\kappa), \tag{34}$$

$$G_{lj}(s) = -\frac{4\pi\sqrt{s}}{m} \frac{f_{lj}(s)}{[g_l(\kappa_0)]^2}, \tag{35}$$

$$f_{lj}(s) = \frac{e^{2i\delta_{lj}(s)} - 1}{2i\kappa_0}, \tag{36}$$

where l and j are the orbital and total angular momentum, respectively, κ_0 is the on-shell momentum evaluated from s, and $\delta_{lj}(s)$ is the phase shift. For the kaon-deuteron scattering, the quantity s in Eq. (34) is taken as

$$s = (W - E_{p_R})^2 - p_R^2, \tag{37}$$

where p_R and E_{p_R} is the momentum and energy of the spectator nucleon. Here the spectator nucleon is assumed to be on-shell. I employ the same off-shell amplitude $\mathcal{M}_{lj}$ used by Garcilazo [8], which is described in what follows. The form of Eq. (35) is used for the physical region $s \geqq (m_K + m)^2$, where m_K is the kaon mass. For the unphysical region $s < (m_K + M)^2$, however, G_{lj} is assumed as

$$G_{lj}(s) = G_{lj}[(m_K + m)^2] \frac{1}{[2 - s/(m_K + m)^2]^2}. \tag{38}$$

The form factor g_l is taken as

$$g_l(\kappa) = \frac{\kappa^l}{(\beta^2 + \kappa^2)^n}, \tag{39}$$

with $\beta = 1$ GeV/c. Here $n = 1$ is used for $l = 0$ and 1, and $n = 2$ is used for $l = 2$ and 3.

For the nucleon-nucleon T matrix, I use the separable form made by means of the Ernst-Shakin-Thaler (EST) method [16]. Because I am mainly interested in the total cross section and integrated elastic cross section at low energies, I take into account only the S-wave contribution in the nucleon-nucleon interaction and disregard the coupling to the D wave. In this work, I employ the separable S-wave NN potential constructed in Ref. [17]. This was obtained by applying the EST method to the Paris potential where the $^3S_1$ state is considered as uncoupled. In this approximation, the nucleon-nucleon T matrix is given as

$$\langle p' | t_{NN}(E_N) | p \rangle = g_N(p') \tau_{NN}(E_N) g_N(p), \tag{40}$$

$$[\tau_{NN}(E_N)]^{-1} = -1 + \frac{\mu}{\pi^2} \int_0^\infty \frac{q^2 [g_N(q)]^2}{q^2 - k_N^2 - i\varepsilon} dq, \tag{41}$$

where $\mu = m/2$, $k_N^2 = 2\mu E_N$, and p (p') is the initial (final) relative momentum of the nucleon-nucleon system. The spin and isospin are again omitted. Here the form factor g_N is defined by $g_N(p) = \sqrt{2\pi^2} g(p)$ in which g is given in Ref. [17]. In this method, the form factor for the $^3S_1$ channel is related to the deuteron wave function as

$$\psi_d(\mathbf{p}) = \frac{2\mu N g_N(p)}{k_B^2 + p^2}, \tag{42}$$

where $k_B^2 = 2\mu E_B$. Here N is a normalization constant.

Now I discuss how the optical potential is evaluated. The first-order optical potential in the kaon-deuteron c.m. frame is written as

$$\begin{aligned}\langle \mathbf{k}'d|U^{(1)}|\mathbf{k}d\rangle &= \langle \mathbf{k}'d|\sum_{i=1}^{2} t_i^{\rm free}|\mathbf{k}d\rangle \\ &= \int \frac{d^3\kappa_d}{(2\pi)^3}\psi_d(\kappa_d')\langle \mathbf{k}'\mathbf{p}_1'|\left[t_p^{\rm free}(s_1)+t_n^{\rm free}(s_1)\right] \\ &\quad\times|\mathbf{k}\mathbf{p}_1\rangle\psi_d(\kappa_d),\end{aligned} \tag{43}$$

where κ_d (κ_d') is the relative momentum of the two-nucleon, $\mathbf{p}_1$ ($\mathbf{p}_1'$) is the momentum of the struck nucleon and the spin of the deuteron is omitted for simplicity. The free kaon-nucleon T matrices $t_p^{\rm free}$ and $t_n^{\rm free}$ describe the processes $K^+p \longrightarrow K^+p$ and $K^+n \longrightarrow K^+n$, respectively, and are evaluated at the invariant mass squared s_1. Here $s_1 = (W - E_{p_2})^2 - p_2^2$ and p_2 is the momentum of the spectator nucleon. The momenta in the integrand are defined in a nonrelativistic way. All of them are given in terms of κ_d, $\mathbf{k}$, and $\mathbf{k}'$ if the momentum conservation law is used. The numerical calculation of Eq. (43) is performed without any factorization. In the energy region I study, the non-spin-flip contributions dominate over the spin-flip contributions in the kaon-nucleon T matrix. Taking account of this fact, the first-order potential with only the S-wave and the non-spin-flip P-wave term is used to solve Eq. (30), while for the spin-flip P-wave term and the D-wave term, the single scattering impulse approximation is used. For the on-shell kaon-nucleon scattering amplitude, I use the phase shifts of Martin [18] or Hyslop *et al.* [19]. Note that the T matrix $t_p^{\rm free}(s_1) + t_n^{\rm free}(s_1)$ in Eq. (43) is expressed as $1/2t_{I=0}^{\rm free}(s_1) + 3/2t_{I=1}^{\rm free}(s_1)$, where $t_{I=0}^{\rm free}$ and $t_{I=1}^{\rm free}$ are $I = 0$ and $I = 1$ isospin T matrices, respectively. This relation indicates that the $I = 1$ KN interaction plays a more important role than the $I = 0$ KN interaction in the K^+d elastic scattering.

The second-order optical potential is constructed with the S-wave kaon-nucleon interaction and the S-wave nucleon-nucleon interaction, because these contributions are expected to be dominant at low energies. In this approximation, thus, the second-order potential is spin-independent. So the spin of the deuteron is suppressed in the following expressions. The double scattering term $U_d^{(2)}$ is written as

$$\begin{aligned}&\langle \mathbf{k}'d|U_d^{(2)}|\mathbf{k}d\rangle \\ &= \langle \mathbf{k}'d|\sum_{i\neq j} t_i^{\rm free}\frac{1}{e_0}t_j^{\rm free}|\mathbf{k}d\rangle \\ &= \int \frac{d^3k''}{(2\pi)^3}\frac{d^3p_r}{(2\pi)^3}\psi_d(\kappa_d')G_0(k'',p_r,k) \\ &\quad\times\Big\{\langle \mathbf{k}'\mathbf{p}_2'|t_p^{\rm free}(s_2)|\mathbf{k}''\mathbf{p}_2\rangle\langle \mathbf{k}''\mathbf{p}_1'|t_n^{\rm free}(s_1)|\mathbf{k}\mathbf{p}_1\rangle \\ &\quad+\langle \mathbf{k}'\mathbf{p}_2'|t_n^{\rm free}(s_2)|\mathbf{k}''\mathbf{p}_2\rangle\langle \mathbf{k}''\mathbf{p}_1'|t_p^{\rm free}(s_1)|\mathbf{k}\mathbf{p}_1\rangle \\ &\quad-\langle \mathbf{k}'\mathbf{p}_2'|t_{ex}^{\rm free}(s_2)|\mathbf{k}''\mathbf{p}_2\rangle\langle \mathbf{k}''\mathbf{p}_1'|t_{ex}^{\rm free}(s_1)|\mathbf{k}\mathbf{p}_1\rangle\Big\}\psi_d(\kappa_d),\end{aligned} \tag{44}$$

where

$$G_0^{-1}(k'',p_r,k) = \omega + \frac{k^2}{4m} - E_B - \omega'' - \frac{k''^2}{4m} - \frac{p_r^2}{m} + i\varepsilon. \tag{45}$$

Here p_r is the relative momentum of two nucleons, and $s_1 = (W - E_{p_2})^2 - p_2^2$ and $s_2 = (W - E_{p_1'})^2 - p_1'^2$, where p_2 and p_1' are the momenta of the spectator nucleon. The free kaon-nucleon T matrix $t_{\rm ex}^{\rm free}$ describes the charge exchange process $K^+n \longrightarrow K^0p$ ($K^0p \longrightarrow K^+n$). The NN scattering term $U_n^{(2)}$ is written as

$$\begin{aligned}&\langle \mathbf{k}'d|U_n^{(2)}|\mathbf{k}d\rangle \\ &= \langle \mathbf{k}'d|\sum_{i,j} t_i^{\rm free}\frac{\mathcal{A}}{e_0}t_{NN}\frac{\mathcal{A}}{e_0}t_j^{\rm free}|\mathbf{k}d\rangle \\ &= \int \frac{d^3k''}{(2\pi)^3}\tau_{NN}[E_N(k'')]\int\frac{d^3p_r'}{(2\pi)^3}\psi_d(\kappa_d')\langle \mathbf{k}'\mathbf{p}_2'| \\ &\quad\times\left[t_p^{\rm free}(s_2)+t_n^{\rm free}(s_2)\right]|\mathbf{k}''\mathbf{p}_2''\rangle G_0(k'',p_r',k)g_N(p_r') \\ &\quad\times\int\frac{d^3p_r}{(2\pi)^3}g_N(p_r)G_0(k'',p_r,k)\langle \mathbf{k}''\mathbf{p}_1''| \\ &\quad\times\left[t_p^{\rm free}(s_1)+t_n^{\rm free}(s_1)\right]|\mathbf{k}\mathbf{p}_1\rangle\psi_d(\kappa_d),\end{aligned} \tag{46}$$

where

$$E_N(k'') = \omega + \frac{k^2}{4m} - E_B - \omega'' - \frac{k''^2}{4m}, \tag{47}$$

and the coherent rescattering term $U_c^{(2)}$ is

$$\begin{aligned}\langle \mathbf{k}'d|U_c^{(2)}|\mathbf{k}d\rangle &= \langle \mathbf{k}'d|\sum_{i,j} t_i^{\rm free}\frac{P}{e}t_j^{\rm free}|\mathbf{k}d\rangle \\ &= \int\frac{d^3k''}{(2\pi)^3}G_c(k'',k)\int\frac{d^3p_r'}{(2\pi)^3}\psi_d(\kappa_d')\langle \mathbf{k}'\mathbf{p}_2'| \\ &\quad\times\left[t_p^{\rm free}(s_2)+t_n^{\rm free}(s_2)\right]|\mathbf{k}''\mathbf{p}_2''\rangle\psi_d(p_r') \\ &\quad\times\int\frac{d^3p_r}{(2\pi)^3}\psi_d(p_r)\langle \mathbf{k}''\mathbf{p}_1''| \\ &\quad\times\left[t_p^{\rm free}(s_1)+t_n^{\rm free}(s_1)\right]|\mathbf{k}\mathbf{p}_1\rangle\psi_d(\kappa_d),\end{aligned} \tag{48}$$

where

$$G_c^{-1}(k'',k) = \omega + \frac{k^2}{4m} - \omega'' - \frac{k''^2}{4m} + i\varepsilon. \tag{49}$$

III. RESULTS

In this section, I discuss the results calculated with the optical potential consisting of the first- and second-order terms. The optical potential is evaluated by taking into account a three-body kinematics fully and without any factorization in the momentum integration. To treat the singularity properly, the usual subtraction procedure is used. As the second-order potential is expected to be important only at low energies, I take into account only the S-wave kaon-nucleon and nucleon-nucleon interactions for it. As the S-wave kaon-nucleon interaction is described by the non spin-flip amplitude, only the NN interaction for the $^3S_1$ channel is included in the calculation of $U_n^{(2)}$. In my calculation, the D-wave NN interaction is ignored for the bound state as well as the intermediate state. This D-wave contribution is important only at the large momentum transfer, as was demonstrated in the calculation of the elastic differential cross sections [6].

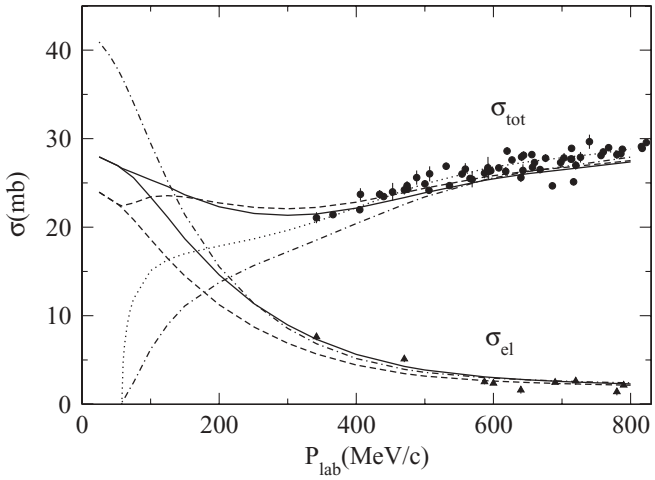

FIG. 1. Total and integrated elastic K^+d cross sections. The solid lines are the results of the full calculation. The dashed and dash-dotted lines are the results of the first-order optical potential and the single scattering impulse approximation, respectively, and the dotted line is the result of Eq. (51). Phase shifts of Martin [18] are used in these calculations. The data of total cross sections are from Refs. [9,20–25] (circles). The data of integrated elastic cross sections are from Refs. [9,26,27] (triangles).

Because the scattering amplitude f_{Kd} at zero- or low-momentum transfer contributes to the total and integrated K^+d elastic cross sections, the D-wave interaction has little effect on them.

Now I show the calculations of the total and integrated elastic cross sections for the K^+d scattering with the experimental data in Fig. 1. Note that some data plotted in Fig. 1 are taken from Table II of Ref. [9], in which the elastic and breakup cross sections are obtained by using both the experimental data [28] and the theoretical values [9]. The cross sections are plotted at incident momenta up to 800 MeV/c. In my calculations, the Coulomb interaction is not included and the K^+N phase shifts of Martin [18] are used. The solid lines correspond to the full calculations including the first- and second-order optical potentials. The agreement with the data is satisfactory for both the total and elastic cross sections. For the total cross section, the theory seems to be small compared with several data at higher energies, but one cannot say that there is a discrepancy between the theory and the data because the data are scattered. The dashed lines are the calculations including only the first-order optical potential. The difference between these two lines shows the size of the second-order potential effect. This effect is most important at lower energies, especially near the threshold. For the total cross section, we find that the second-order potential effect decreases its magnitude slightly at $P_{\rm lab} \gtrapprox 150$ MeV/c, but it increases at $P_{\rm lab} \lessapprox 150$ MeV/c. For the integrated elastic cross section, this effect increases it and such tendency becomes stronger as the energy is lower. Generally speaking, the second-order potential effect is more important for the elastic cross section than the total one but it is small at $P_{\rm lab} \gtrapprox 500$ MeV/c for both cases. The dash-dotted lines correspond to the calculations of the single scattering impulse approximation where the transition amplitude $T_{\rm IA}$ is given as

$$T_{\rm IA} = \langle \mathbf{k}' d | U^{(1)} | \mathbf{k} d \rangle. \tag{50}$$

In this approximation, the unitarity is explicitly violated at low momenta, where the elastic cross section is larger than the total cross section, as shown in Fig. 1. By comparing the dash-dotted and dashed lines, we find that the coherent rescattering effect has a significant contribution for both the total and the elastic cross sections at momenta below ∼500 MeV/c and drastically changes the size of cross sections at low energies so as to recover the unitarity. I consider further approximation to the total cross section. I calculate it by factorizing the kaon-nucleon T matrix $t_i^{\rm free}$ out of the integral of Eq. (43). Here the T matrix is evaluated at $\mathbf{p}_1 = -\mathbf{k}/2$ and its form factor is taken to be $g_l = 1$. Using the optical theorem, one gets

$$\sigma^{\rm tot}_{K^+d} = K\left(\sigma^{\rm tot}_{K^+p} + \sigma^{\rm tot}_{K^+n}\right), \tag{51}$$

with

$$K = \frac{k_0\sqrt{s_0}E_d}{kE_{k/2}W}, \tag{52}$$

$$k_0^2 = \frac{\left(s_0 - m_K^2 - m^2\right)^2 - 4m_K^2 m^2}{4s_0}, \tag{53}$$

where $s_0 = (W - E_{k/2})^2 - k^2/4$ and the kinematical factor K approaches unity at higher energies. The dotted line is plotted using Eq. (51) and is in good agreement with the data. The difference between this line and the dash-dotted line shows the size of the Fermi motion effect which comes from the energy dependence of the kaon-nucleon amplitude. This effect decreases the magnitude of the cross section. Thus, the single scattering impulse approximation underestimates the total cross section at momenta below ∼500 MeV/c. However, because the data of the total cross sections are rather scattered, all calculations including the full calculation are consistent with the data at momenta above ∼500 MeV/c.

To examine the validity of my approach, I compare my full calculation with the Faddeev calculation by Garcilazo [8]. Because there are no data at momenta below 342 MeV/c, I regard the results of the Faddeev calculation as the data. I use the same kaon-nucleon T matrix used in Ref. [8] but consider only the isospin $I = 0$ S-wave nucleon-nucleon interaction as already mentioned. As the incident momentum gets smaller, the Coulomb effect becomes non-negligible. However, it is meaningful to make a comparison between my calculation and the Faddeev calculation [8] because the Coulomb interaction is neglected in both calculations and the two-body interactions used are almost the same. The results are shown in Fig. 2. The solid, dashed, and dash-dotted lines correspond to my full calculations for the total, integrated elastic, and integrated inelastic cross sections, respectively. The integrated inelastic cross section $\sigma_{\rm inel}$ is given by $\sigma_{\rm inel} = \sigma_{\rm tot} - \sigma_{\rm el}$. The open circles, open triangles, and open squares correspond to the Faddeev calculations [8,9] for the total, integrated elastic, and integrated inelastic cross sections, respectively. The open symbols at the threshold are taken from Fig. 1 of Ref. [8]. The solid symbols are the corresponding data given in Table II of Ref. [9]. My calculations are in good agreement with the Faddeev calculations as well as the data.

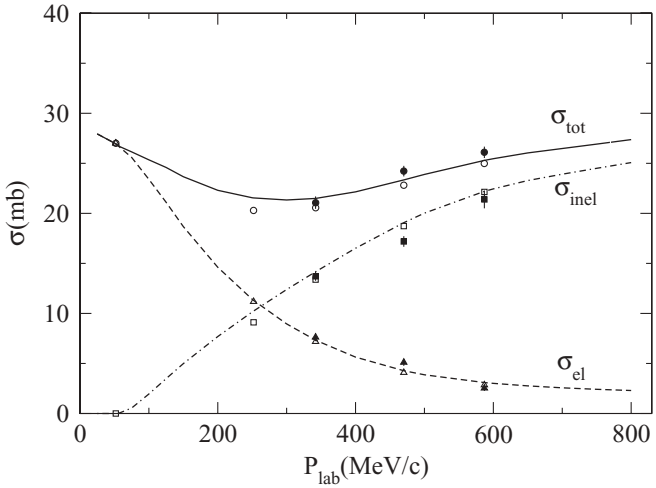

FIG. 2. Total (solid line), integrated elastic (dashed line), and integrated inelastic (dash-dotted line) K^+d cross sections given by my full calculations. The open symbols correspond to the Faddeev calculation [8,9]. The data are from Ref. [9] (solid symbols). The circles, triangles, and squares denote the total, integrated elasic, and integrated inelastic cross sections, respectively.

The maximum discrepancy between my calculation and the Faddeev calculation is 6% at 252 MeV/c for the total cross section and 8% at 587 MeV/c for the elastic cross section. These results demonstrate that my model, where the optical potential contains both the first- and second-order terms, is good enough to describe these cross sections.

To see how my method predicts the elastic differential cross sections, the calculations at three incident momenta are presented with the data in Fig. 3. The solid, dashed, and dash-dotted lines correspond to the full calculation, the calculation with the first-order optical potential, and the single scattering impulse approximation, respectively. Because the D-wave contribution in the NN interaction is disregarded, all calculations at the backward angles are naturally underestimated. We find that the second-order optical potential makes the cross section increase and brings it close to the data at backward angles. For the forward angles, however, my full calculation is roughly consistent with the measurement as well as the Faddeev calculation shown in Figs. 2–4 of Ref. [8]. The Coulomb interaction is again ignored in these calculations because its effect is expected to be small except for the very forward angles where there are no measurements. However, it will be necessary to take into account the Coulomb interaction when one calculates the cross sections at the lower momentum transfer or at the lower incident momentum or for the heavier nucleus. The theoretical treatment of the Coulomb force is not difficult in my approach because the optical potential necessary is obtained by simply adding the Coulomb potential to the strong optical potential [12].

To see the effects of the multiple scattering, I have calculated the total and integrated elastic cross sections using several different types of the optical potential. The results are shown in Fig. 4. The solid and dashed lines correspond to the results evaluated with $U^{(1)} + U^{(2)}$ and $U^{(1)}$, respectively. These lines are the same as in Fig. 1. The dash-dot-dotted and dotted lines

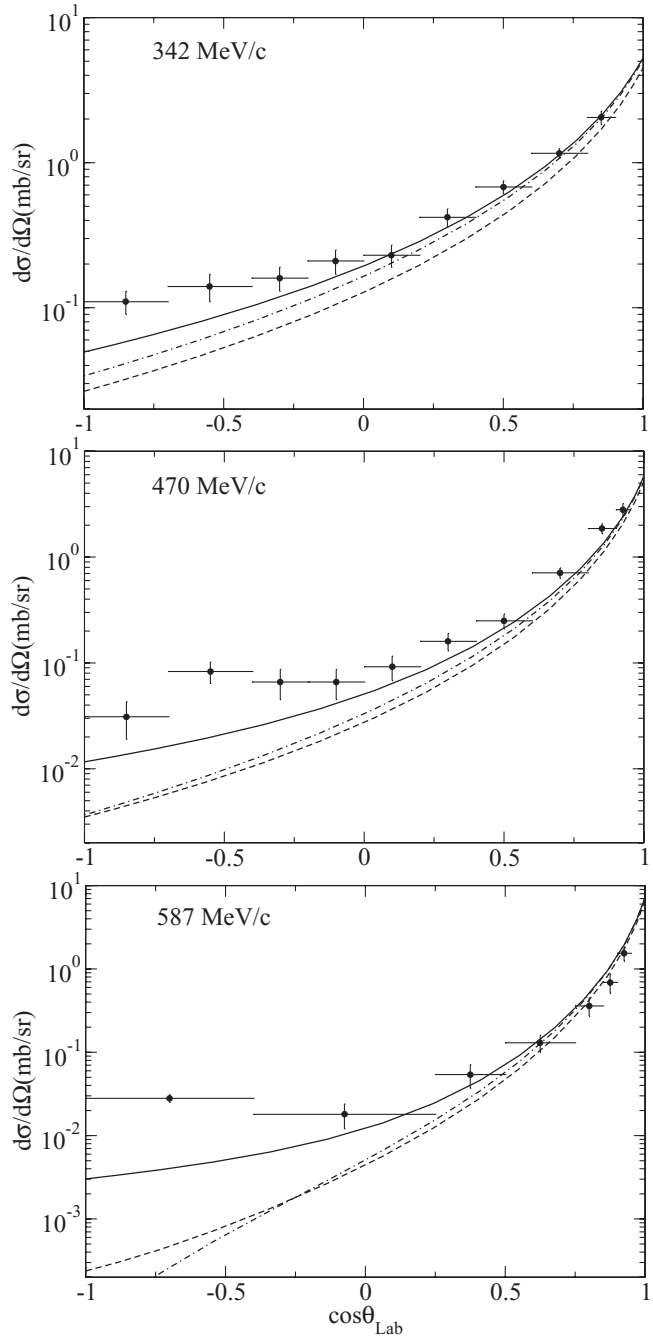

FIG. 3. K^+d elastic differential cross sections at three incident momenta. The solid line is the result of the full calculation. The dashed and dash-dotted line are the results of the first-order potential and the single scattering impulse approximation, respectively. The data are from Ref. [28].

are the calculations with $U^{(1)} + U_d^{(2)}$ and $U^{(1)} + U_n^{(2)} - U_c^{(2)}$, respectively. The quantities $U_d^{(2)}$ and $U_n^{(2)} - U_c^{(2)}$ represent the effects of the double scattering and the modified NN scattering, respectively. From the comparison of the dashed line with the dash-dot-dotted line or the dotted line, we can see the size of the multiple scattering effects. Although the effects of the double scattering and the modified NN scattering are negligible at higher momenta than 600 MeV/c, they become

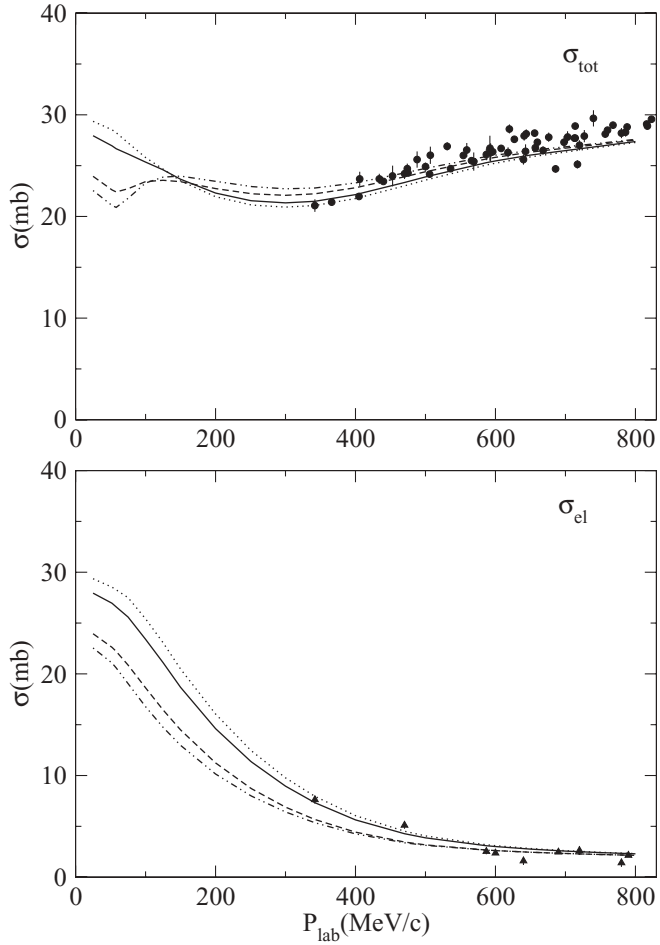

FIG. 4. Total (top) and integrated elastic (bottom) K^+d cross sections. The solid and dashed lines are the results of the full calculation and the first-order optical potential, respectively. The dash-dot-dotted and dotted lines are the results of the calculation with the the double scattering effect and the modified NN scattering effect, respectively. See the details in the text. The data are the same as Fig. 1.

important with the decreasing of momentum. In the case of the total cross section shown in the top diagram of Fig. 4, the double scattering term increases the cross section shown by the dashed line and the modified NN scattering term decreases it, but at momenta lower than $\sim$100 MeV/c, the effect of the two terms is completely opposite. Near the threshold, furthermore, all lines agree with the corresponding lines in the bottom diagram of Fig. 4. In the case of the elastic cross section, however, the double scattering term decreases the cross section shown by the dashed line and the modified NN scattering term increases it. We also find that the effect of the modified NN scattering term is larger than that of the double scattering term.

So far I have used the K^+N phase shifts of Martin [18] to compare my calculation with the Faddeev calculation by Garcilazo [8] and check the validity of my method. Here I examine the dependence of the one-shell K^+N amplitude. In Fig. 5, I show the cross sections calculated by using the phase shifts of Hyslop *et al.* [19]. At $P_{\rm lab} > 500$ MeV/c, the calculation is in good agreement with the data. However,

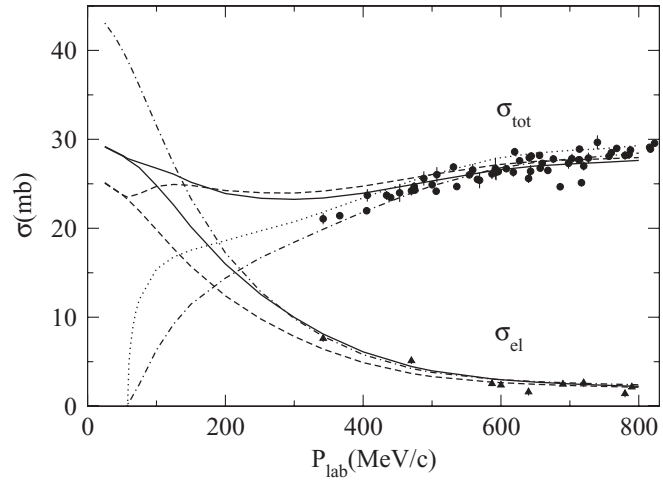

FIG. 5. The same as Fig. 1, except that the theoretical curves are calculated using the phase shifts of Hyslop *et al.* [19].

at $P_{\rm lab} \approx 400$ MeV/c, the full calculation for the total cross section does not agree with the data. Such discrepancy can be understood from the comparison of the total cross sections given by Eq. (51) (see the dotted lines in Figs. 1 and 5). The total cross section represented by the dotted line in Fig. 5 is slightly larger than that in Fig. 1, although both of the lines almost agree with the data. Once the effects of the multiple scattering and the Fermi motion are included in the calculation, however, this tendency leads to a significant difference between the two calculations of the total cross sections shown in Figs. 1 and 5.

IV. CONCLUSIONS

The single scattering impulse approximation is able to describe the K^+d data at incident momenta above $\sim$500 MeV/c but explicitly violates the unitarity below 200 MeV/c and furthermore fails to explain the breakup reaction cross section at the forward kaon scattering angles. Accordingly, the single scattering impulse approximation is not satisfactory for explaining the K^+d scattering. My purpose was to examine how consistently the optical potential describes the K^+d scattering. This approach does not violate the unitarity unless an unphysical potential is used. Another advantage of the optical potential is that the calculation is straightforward compared with the Faddeev method.

I constructed the optical potential consisting of the first- and second-order terms. The second-order optical potential includes the double scattering term and the modified NN scattering term. The first- and second-order potentials were evaluated without any factorization in the momentum integration. This potential was used to calculate the total, integrated elastic, and elastic differential cross sections at incident momenta below 800 MeV/c. I found that my optical potential approach is able to explain both the Faddeev calculation and the data consistently and especially that the second-order optical potential plays an essential role at low energies.

It was demonstrated in my calculations that the multiple scattering effects such as the coherent rescattering, the double

scattering and the modified NN scattering have an important contribution to the cross sections at low energies despite the weak K^+N interaction. This importance may be related to the fact that the wavelength of K^+ is comparable to the distance between two nucleons in the deuteron. At low energies, therefore, the multiple scattering effects should be taken into account when one extracts the on-shell K^+N amplitudes from the K^+d data. This was confirmed through the comparison of the calculations obtained using two kinds of K^+N phase shifts.

It is interesting to examine whether my approach is applicable for other reactions arising from the strong elementary interaction such as a πd scattering and a K^-d scattering. Furthermore, my optical potential approach could be used to study the effect of the pentaquark resonance $\Theta(1540)$ in the K^+d scattering and especially to learn how the effects of the multiple scattering affect the suppression of the resonance peak in the K^+d cross sections.

My optical potential has been derived from the Watson multiple scattering theory. Similarly, the optical potential up to second order can be formulated based on the KMT multiple scattering theory, as shown in the Appendix. We have numerically tested the difference between two approaches. Within the first-order optical potential approach, the result using the Watson formulation does not agree with that using the KMT formulation. In the latter calculation, the integrated elastic cross section becomes larger than the total cross section at low momenta. This does not mean that the imaginary part of the KMT first-order optical potential is positive at low energies, but this is attributable to the factor $\frac{A-1}{A}$ in the KMT formulation. When the second-order optical potential is taken into account, however, the two approaches give almost identical cross sections. It was found from my numerical estimate that the difference was a few percent or less except near the threshold. Therefore, my conclusions in this article are not changed by which formulation is chosen.

ACKNOWLEDGMENT

The author thanks M. Hirata for useful discussions.

APPENDIX

I derive the optical potential from the KMT multiple scattering theory. The transition amplitude T of Eq. (1) is rewritten as

$$T = \sum_{i=1}^{A} T_i, \tag{A1}$$

where

$$T_i = \tau_i + \tau_i \frac{\mathcal{A}}{e} \sum_{j \neq i} T_j, \tag{A2}$$

$$\tau_i = v_i + v_i \frac{\mathcal{A}}{e} \tau_i. \tag{A3}$$

To get the KMT optical potential $U_{\rm KMT}$, I introduce the operator $\tilde{U}_i$ defined by

$$T_i = \tilde{U}_i + \tilde{U}_i \frac{P}{e} \sum_{j \neq i} T_j. \tag{A4}$$

In the KMT formulation, all equations are derived in the antisymmetric subspace of the Hilbert space. Consequently, the operators of τ_i, $\tilde{U}_i$, and T_i are independent of i. With the help of the relation $\sum_{j \neq i} T_j = \frac{A-1}{A} T$, Eq. (A4) can be expressed as

$$T' = U_{\rm KMT} + U_{\rm KMT} \frac{P}{e} T', \tag{A5}$$

where

$$T' = \frac{A-1}{A} T, \tag{A6}$$

$$U_{\rm KMT} = \frac{A-1}{A} \sum_{i=1}^{A} \tilde{U}_i. \tag{A7}$$

Similarly, Eq. (A2) is written as

$$T' = \tau_{\rm KMT} + \tau_{\rm KMT} \frac{\mathcal{A}}{e} T', \tag{A8}$$

where

$$\tau_{\rm KMT} = \frac{A-1}{A} \sum_{i=1}^{A} \tau_i. \tag{A9}$$

The scattering operator T is obtained by solving Eq. (A5), if the optical potential $U_{\rm KMT}$ is given. With the help of Eqs. (A5) and (A8), the operator $U_{\rm KMT}$ can be written in terms of τ_i as

$$U_{\rm KMT} = \tau_{\rm KMT} + \tau_{\rm KMT} \frac{Q}{e} U_{\rm KMT} \tag{A10}$$

$$= \frac{A-1}{A} \sum_{i=1}^{A} \tau_i + \frac{A-1}{A} \sum_{i=1}^{A} \tau_i \frac{Q}{e} U_{\rm KMT}. \tag{A11}$$

Now I build the first-order and second-order optical potentials using Eq. (A11). The operator τ_i can be written in terms of t_i as Eq. (10) in Sec. II. Here the operator t_i is defined by Eq. (8). By substituting Eq. (10) into Eq. (A11), the operator $U_{\rm KMT}$ can be expressed in terms of t_i as

$$U_{\rm KMT} = \frac{A-1}{A} \left(\sum_i t_i + \sum_{i \neq j} t_i \frac{1}{e} t_j - \sum_{i \neq j} t_i \frac{P}{e} t_j + \cdots \right). \tag{A12}$$

Note that an intermediate state in the operators $U_{\rm KMT}$ and t_i is either an antisymmetric state or a non-antisymmetric state. Equation (A12) displays the KMT optical potential to second order in t_i, which corresponds to the Watson optical potential of Eq. (13). Now I consider the optical potential $U_{\rm KMT}$ used in the calculation of the K^+d scattering. Using the same procedure mentioned in Sec. II, we obtain the final expression,

$$U_{\rm KMT} = U^{(1)}_{\rm KMT} + U^{(2)}_{\rm KMT} + \cdots, \tag{A13}$$

with

$$U^{(1)}_{\rm KMT} = \frac{1}{2} U^{(1)}, \tag{A14}$$

$$U^{(2)}_{\rm KMT} = \frac{1}{2} \left[U^{(2)} + \sum_i t_i^{\rm free} \frac{P}{e} t_i^{\rm free} \right], \tag{A15}$$

where the operators $U^{(1)}$, $U^{(2)}$, and $t_i^{\rm free}$ are defined in Sec. II.

[1] T. Nakano *et al.*, Phys. Rev. Lett. **91**, 012002 (2003).
[2] T. Nakano *et al.*, Phys. Rev. C **79**, 025210 (2009) , and references therein.
[3] R. N. Cahn and G. H. Trilling, Phys. Rev. D **69**, 011501(R) (2004).
[4] W. R. Gibbs, Phys. Rev. C **70**, 045208 (2004).
[5] A. Sibirtsev, J. Haidenbaur, S. Krewald, and Ulf-G. Meißner, Phys. Lett. B **599**, 230 (2004).
[6] A. Sibirtsev, J. Haidenbaur, S. Krewald, and Ulf-G. Meißner, J. Phys. G **32**, R395 (2006).
[7] V. E. Tarasov, V. V. Khabarov, A. E. Kudryavtsev, and V. M. Weinberg, Phys. At. Nucl. **71**, 1410 (2008).
[8] H. Garcilazo, Phys. Rev. C **37**, 2022 (1988).
[9] H. Garcilazo, Phys. Rev. C **44**, 966 (1991).
[10] K. M. Watson, Phys. Rev. **89**, 575 (1953).
[11] A. K. Kerman, H. McManus, and R. M. Thaler, Ann. Phys. (NY) **8**, 551 (1959).
[12] R. Nagaoka and K. Ohta, Phys. Rev. C **33**, 1393 (1986).
[13] I. R. Afnan and A. T. Stelbovics, Phys. Rev. C **23**, 845 (1981).
[14] H. Garcilazo and G. Mercado, Phys. Rev. C **25**, 2596 (1982).
[15] M. Hirata, F. Lenz, and K. Yazaki, Ann. Phys. (NY) **108**, 116 (1977).
[16] D. J. Ernst, C. M. Shakin, and R. M. Thaler, Phys. Rev. C **8**, 46 (1973).
[17] H. Zankel, W. Plessas, and J. Haidenbauer, Phys. Rev. C **28**, 538 (1983).
[18] B. R. Martin, Nucl. Phys. B **94**, 413 (1975).
[19] J. S. Hyslop, R. A. Arndt, L. D. Roper, and R. L. Workman, Phys. Rev. D **46**, 961 (1992).
[20] T. Bowen *et al.*, Phys. Rev. D **2**, 2599 (1970).
[21] T. Bowen *et al.*, Phys. Rev. D **7**, 22 (1973).
[22] A. S. Carrol *et al.*, Phys. Lett. B **45**, 531 (1973).
[23] G. Giacomelli *et al.*, Nucl. Phys. B **37**, 577 (1972).
[24] D. V. Bugg *et al.*, Phys. Rev. **168**, 1466 (1968).
[25] R. A. Krauss *et al.*, Phys. Rev. C **46**, 655 (1992).
[26] G. Giacomelli *et al.*, Nucl. Phys. B **68**, 285 (1974).
[27] M. Sakitt *et al.*, Phys. Rev. D **12**, 3386 (1975).
[28] R. G. Glasser *et al.*, Phys. Rev. D **15**, 1200 (1977).